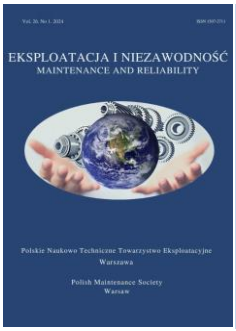

Eksploatacja i Niezawodnosc – Maintenance and Reliability
Volume 26 (2024), Issue 1
journal homepage: http://www.ein.org.pl

Article citation info:
Yan Y, Zhou J, Yin Y, Nie H, Wei X, Liang T, Reliability Estimation of Retraction Mechanism Kinematic Accuracy under Small Sample, Eksploatacja i Niezawodnosc – Maintenance and Reliability 2024: 26(1) http://doi.org/10.17531/ein/174777

Reliability Estimation of Retraction Mechanism Kinematic Accuracy under Small Sample

Indexed by:

Yumeng Yan[a], Jiyuan Zhou[a], Yin Yin[a,*], Hong Nie[a], Xiaohui Wei[a], Taotao Liang[b]

[a] State Key Laboratory of Mechanics and Control for Aerospace Structures, Nanjing University of Aeronautics and Astronautics, China
[b] Nanjing University of Aeronautics and Astronautics, College of General Aviation and Flight, China

Highlights

- A Bayesian-based reliability analysis method fusing prior and test data is proposed.
- The prior data are expanded using the neural network in combination with simulation data.
- The mechanism kinematic accuracy reliability is quantified under small-sample conditions.
- The key variables affecting the retraction mechanism reliability are identified.

Abstract

Due to intricate operating conditions, including structural clearances and assembly deviations, the acquisition of test data for the landing gear retraction mechanism is limited, posing challenges for reliability analysis. To solve the problem, a Bayesian-based reliability analysis method fusing prior and test data is proposed, focusing on the mechanism kinematic accuracy under small-sample conditions. Firstly, a dynamic simulation model is established to collect prior data, and retraction tests are conducted to obtain test data. Then, based on Bayesian theory, the motion accuracy parameter estimation model integrating prior and test samples is established. To obtain accurate hyper parameters, the prior samples are expanded using the neural network. Finally, taking the retraction mechanism as the research object, the kinematic accuracy reliability is quantified, and the impact of uncertainty factors is analysed in depth. The results show that the proposed method is superior to the classical interval estimation method in stability and effectively mitigates the impact of uncertainty factors.

Keywords
Bayesian, small sample, retraction mechanism, kinematic reliability, hyper parameter estimation

1. Introduction

In order to verify the motion principle of the mechanism, expose the design defects and faults, and eliminate the potential failure factors, it is crucial to conduct reliability testing and motion reliability analysis of the landing gear retraction mechanism. The landing gear retraction system is a complex system that integrates mechanism dynamics, hydraulic dynamics, and electronic control [4]. However, due to cost and time limitations, the landing gear retraction test can only be performed with limited samples [10,18]. The kinematic accuracy of the retraction mechanism is influenced by various factors, such as joint clearance and assembly deviation, which introduce uncertainties in the process of design, manufacture, and use [17,28]. These uncertainties make it more challenging to accurately characterize the actual distribution of the kinematic accuracy parameters of the mechanism based on small-sample tests. Consequently, it can be tough to assess the accurate and stable reliability, and the credibility of the results is constrained. To address this issue, it is essential to develop a reliability estimation approach specifically tailored to the motion characteristics of the retraction mechanism under the condition

(*) Corresponding author.
E-mail addresses: Y. Yan (ORCID: 0009-0004-0341-3158) yanyumeng@nuaa.edu.cn, J. Zhou (ORCID: 0009-0009-0144-6219) jiyuanzhou@nuaa.edu.cn, Y. Yin (ORCID: 0009-0004-0752-3039) yinyin@nuaa.edu.cn, H. Nie hnie@nuaa.edu.cn, X. Wei wei_xiaohui@nuaa.edu.cn, T. Liang (ORCID: 0000-0001-5355-0856) liangtt@nuaa.edu.cn,

of small sample.

In response to the challenge of limited test samples in mechanism reliability analysis, Yin et al. [27] constructed the response surface using sample data derived from the mathematical model and investigated the impact of key parameters on the reliability of the retraction mechanism. To improve the computational efficiency of reliability analysis, Hu et al. [13] introduced the advanced adaptive Kriging model based on the multi-body dynamic simulation model of the adjusting mechanism of tail nozzle. Wang et al. [25] proposed a robot reliability analysis method based on the dynamic mathematical model considering multiple failure modes, and fitted the experimental data by neural network to verify the validity of the theoretical analysis with the reliability results obtained.

The above paper did not directly use experimental information, but relied on prior information (such as expert experience, historical data, and simulation data) to estimate the distribution of performance characteristic parameters. These estimates may not accurately capture the characteristics of new products, potentially affecting the accuracy of reliability estimation results. Furthermore, the classical interval estimation method estimates a range of possible values of performance characteristic parameters based on test data. Li et al. [12] proposed an improved interval estimation method based on Bootstrap and applied it to the interval estimation of reliability parameters of the NC machine tools under different working conditions. Similarly, Li et al. [16] utilized the parameter Bootstrap method for the interval estimation of reliability parameters in the context of rolling bearings within an intelligent tool changing robot system. However, it is important to note that due to the dynamics and uncertainty of the test process, the small sample test data may not belong to the same population in essence, resulting in considerable risk in the interval estimation results [15].

In order to enhance the analysis methodology, the Bayesian method is employed to fuse the experimental information and prior information, enabling more robust statistical inference of kinematic accuracy parameters. Consequently, the stability and accuracy of the kinematic reliability evaluation results for the mechanism under small-sample test conditions are improved. Aiming at the characteristics of the small sample test data of the orbital components and the residual life following the Weibull distribution, Zhao et al. [30] proposed a method that incorporates multi-source information (including historical lifetime data, degradation data, expert information, similar data, etc.) based on the Bayesian method to evaluate the residual life of the on-orbit satellite orbital components, which enhanced the robustness of the evaluation results. Based on the Bayesian method, Peng et al. [21] developed a reliability evaluation model for CNC system based on multi-source information fusion, thereby mitigating errors arising from small-sample conditions. Furthermore, utilizing failure data of different environmental characteristics, Wei et al. [22] established a failure rate prediction model for electrical meters under small-sample conditions using the weighted hierarchical Bayesian approach.

However, it is challenging to ensure the accuracy and robustness of the aforementioned methods when there is insufficient prior information. Additionally, the existing literature mainly focuses on the application of the Bayesian method in the field of product failure rate, lifetime, and degradation parameter prediction under small-sample conditions. There is currently a dearth of study on the accuracy and robustness of product kinematic accuracy parameters under small-sample conditions.

In addressing the aforementioned issues, this paper contributes in the following ways: 1) This study extensively leverages information in the design and testing phases of the mechanism. By effectively integrating prior data with experimental data, this study offers a robust framework for evaluating the reliability of retraction mechanism under small-sample conditions. 2) The prior information used in this research is derived from a high-precision dynamic simulation model. To enhance computational efficiency, the neural network method is employed to augment the simulation data. Additionally, the study ensures the accuracy and stability of prior data through rigorous stationarity analysis, thereby guaranteeing the quality of prior information. These contributions collectively advance the assessment of mechanism reliability under the constraints of small-sample testing conditions.

In this paper, Section 2 focuses on establishing the dynamic simulation model that takes joint clearance and assembly

deviation into consideration. Retraction tests are conducted to verify the accuracy of the simulation model, providing data support for reliability estimation. Based on the failure characteristics of the retraction mechanism, the kinematic accuracy reliability model of the retraction mechanism is established. Moving to Section 3, a kinematic accuracy parameter estimation method is proposed, that integrates prior information and experimental data using the Bayesian approach. In Section 4, with the aid of the neural network, the prior data is expanded using simulation data to overcome the limitation of insufficient prior information. The kinematic accuracy reliability estimation process is then established by combining this approach with the reliability calculation method. In Section 5, the proposed parameter estimation method is applied to obtain the kinematic accuracy parameter distribution for the retraction mechanism. The efficiency and stability of the proposed method are evaluated through a comparative analysis with the classical interval estimation method. Subsequently, the kinematic accuracy reliability of the retraction mechanism is calculated, and the key variables affecting reliability are identified. Conclusions are made in Section 6.

2. Retraction mechanism dynamics and reliability model

2.1. Function definition of retraction mechanism

The present study focuses on the dynamic modeling of a novel and intricate landing gear retraction mechanism specifically designed to accommodate the rotatable wheel.

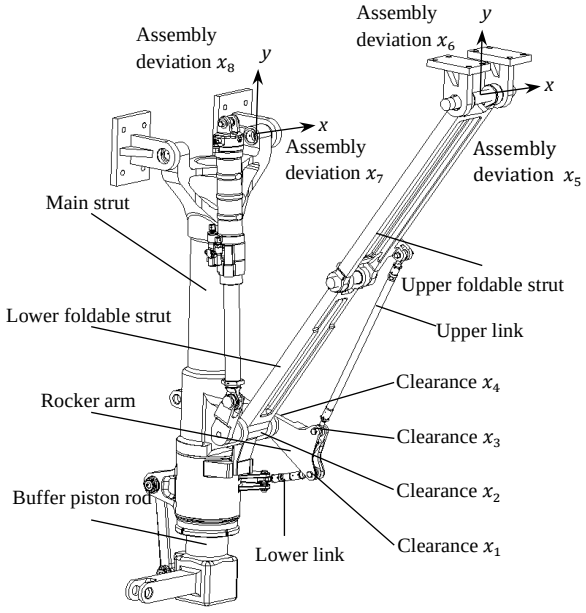

Fig. 1. Landing gear retraction mechanism.

The three-dimensional model of the retraction mechanism is shown in Fig. 1. During the retraction process, the actuator cylinder drives the main strut to rotate. Subsequently, the rotational motion is transmitted to the wheel via a series of interconnected components, including the lower foldable strut, upper foldable strut, upper link, rocker arm, and lower link. This coordinated motion enables the wheel, which is mounted on the buffer piston rod, to rotate accordingly.

As depicted in Fig. 2(a), when the landing gear is fully retracted to its predetermined position, the primary objective of the retraction mechanism is to achieve a flat orientation of the wheel, ensuring a specific safety distance denoted as ‘d’ between the wheel and the cabin door. This configuration effectively minimizes the vertical space occupied by the landing gear within the aircraft cabin. It’s crucial to emphasize that the main strut of the retraction mechanism is locked in an upper position, meaning that the retraction angle remains fixed. Consequently, the distance between the wheel and the cabin door is directly correlated with the rotation angle of the buffer piston rod. The allowable maximum distance between the wheel and the cabin door corresponds directly to the rotation limit error of the buffer piston rod. It is through this relationship that the value of the kinematic accuracy threshold is determined.

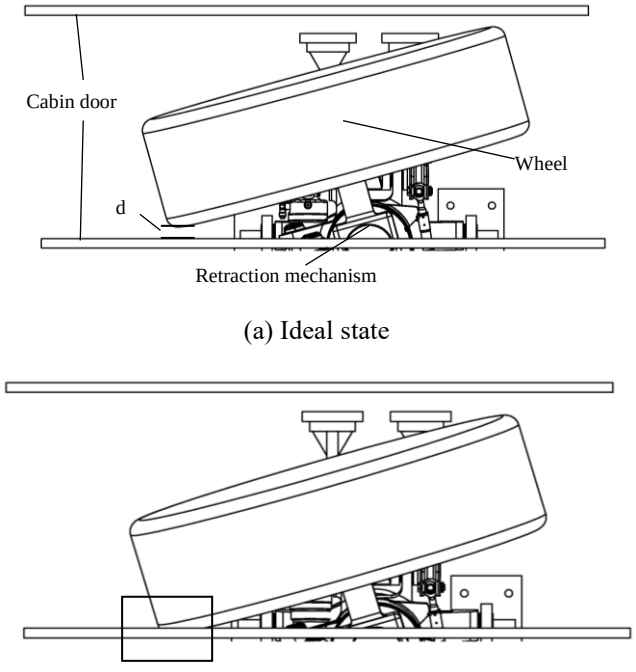

(a) Ideal state

(b) Interference state

Fig. 2. The relative position of the wheel and landing gear cabin door.

Throughout the operation of the retraction mechanism, the motion trajectory of each component will inevitably be affected by uncertain factors such as joint clearance and initial assembly deviation, resulting in motion errors. Under the cumulative effect of motion errors generated by each individual component, when the landing gear is retracted to the designated angle, the motion error of the buffer piston rod exceeds the acceptable threshold. Consequently, an interference situation arises between the rotatable wheel and the cabin door, as depicted in Fig. 2(b). In this instance, the kinematic accuracy of the retraction mechanism fails to meet the specified requirements.

2.2. Dynamics simulation model of retraction mechanism

Using the LMS Virtual.Lab Motion simulation software, referred to as Motion, the dynamic model of the retraction mechanism is established based on the landing gear retraction principle. This process involves four key steps: simplify the landing gear retraction mechanism model; assign quality attributes to each component; establish motion pairs and the constraints between components; apply load.

Considering the impact of structural clearances and assembly deviations on the kinematic accuracy of the retraction mechanism, the structural clearance model for the four critical clearance locations, as shown in Fig. 1, is developed. Additionally, the assembly deviation model for the mounting positions of the main strut and upper foldable strut is developed. The approach for modeling structural clearances involves using multiple sphere-to-plane contact models to simulate the clearances between holes and shafts. Furthermore, to constrain the axial freedom of the shafts at these contact points, point-surface high pairs have been introduced. To simulate assembly deviations in both horizontal and vertical directions, dummy objects are introduced on the ear plate, the moving pairs between these objects and the ear plate are implemented, and the motion pair driver is applied. Both the structural clearances and assembly deviations are parameterized to capture their variability. The simulation diagram of the clearance between the upper link and the rocker arm is shown in Fig. 3, while the simulation diagram of the assembly deviation of the main strut is shown in Fig. 4.

Taking into account the structural flexibility characteristics, the foldable strut, link, and rocker arm undergo a flexibility treatment using Hypermesh software. Subsequently, the flexibility files are imported into Motion. The rigid-flexible coupling dynamic simulation model is obtained, as depicted in Fig. 5. Utilizing this model for batch simulations provides the rotation angle of the buffer piston rod concerning changes in the retraction angle of the main strut under various operating conditions. With appropriate data preprocessing, the rotation output error of the buffer piston rod can be obtained.

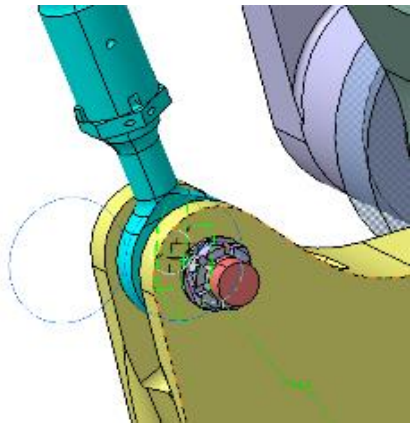

Fig. 3. The clearance between the upper link and the rocker arm.

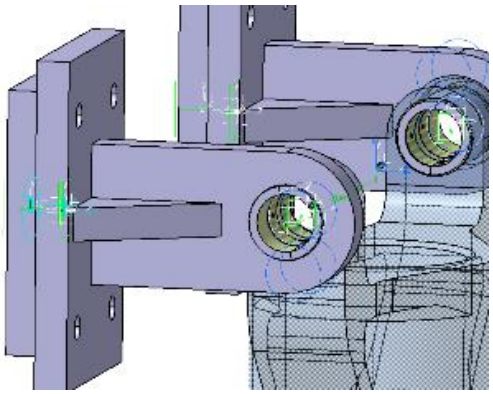

Fig. 4. The installation deviation of the main strut.

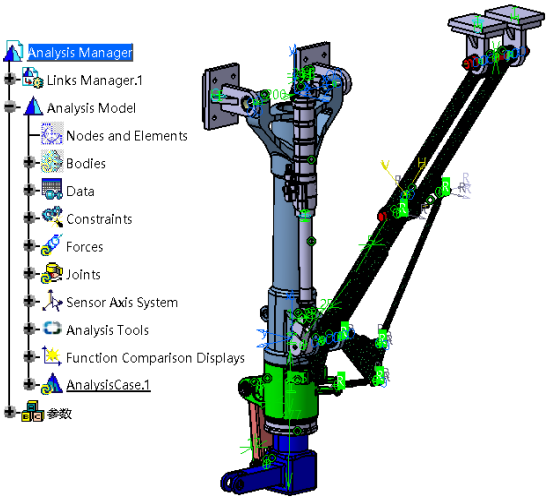

Fig. 5. Dynamics simulation model of retraction mechanism.

2.3. Dynamics test of retraction mechanism

The structural clearance of the retraction mechanism is simulated by replacing the bolts with different sizes, and the assembly deviation is simulated by setting the adjustable fixture. Subsequently, the retraction mechanism is subjected to testing under different working conditions to evaluate its performance. The experimental prototype of the retraction mechanism is shown in Fig. 6.

Fig. 6. Retraction mechanism experimental prototype.

As depicted in Fig. 1, there are eight key factors affecting the mechanism's performance, namely four structural clearances and four assembly deviations. Three different sizes of structural clearances and assembly deviations need to be simulated in the test. If the full factorial design is used for the test, it needs to be carried out under 3^8 working conditions. Such a large-scale experiment would not only consume extensive testing time to disassemble and reassemble the retraction mechanism repeatedly but also introduce the potential for human-induced errors that could degrade the mechanism's kinematic accuracy. To reduce the test cost, it becomes necessary to select a subset of representative working conditions for the test while collecting data. Consequently, the data obtained from this small-sample test may not accurately represent the actual distribution of the mechanism's kinematic accuracy parameters.

To address this issue, the experimental data is used to refine the dynamic simulation model of the retraction mechanism, ensuring the accuracy of the simulation model. Subsequently, a data fusion approach integrating the experimental data with simulation data is employed to estimate the distribution parameters of the mechanism's kinematic accuracy. As shown in Fig. 7, the motion trajectory of the retraction mechanism obtained from simulation is compared with the experimental results in the initial state. The curve depicting the variation of the retraction angle of the mechanism with the rotation angle of the wheel shows a close agreement between the simulation and experimental data. The relative error between them is less than 1×10^{-3}, indicating that the accuracy of the simulation model meets the required level.

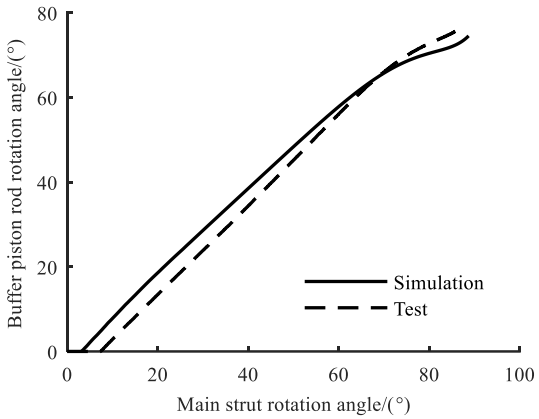

Fig. 7. Comparison of simulation data and test data.

2.4. Reliability model of retraction mechanism

The retraction time of the mechanism is 4 to 7 seconds, and it accounts for a relatively small proportion of the entire landing gear lifecycle. Therefore, it is assumed that the mechanism does not experience performance degradation during this single retraction cycle. The performance function corresponding to the failure mode of the kinematic accuracy of the retraction mechanism is expressed as

$$Z(\boldsymbol{X}) = g(\boldsymbol{X}) = \Delta^* - \Delta \tag{1}$$

wherein, $\boldsymbol{X} = [x_1, x_2, \ldots, x_r]$ is made up of random variables that affect the kinematic precision function of the retraction mechanism, the distribution information is shown in Table 1. The specific locations of the clearance at the joint of the components and the installation deviation at the connection between the components and the fuselage in the retraction mechanism are shown in Fig. 1. Δ^* is expressed as the rotation limit error of the buffer piston rod, that is, the kinematic accuracy threshold given by the design. Δ is expressed as the rotation output error of the buffer piston rod, that is, the kinematic accuracy parameter measured by the test data. When $\Delta^* \geq \Delta$, the kinematic error of the retraction mechanism falls within the allowable range, it is concluded that the retraction mechanism meets the specified kinematic accuracy criteria.

Table 1. The distribution of random variable.

Parameters/(mm)	Distributions	Parameters/(mm)	Distributions
Joint clearance between lower link and rocker arm x_1	$N(u_{x_1}=0.039,\sigma_{x_1}^2=0.007^2)$	Joint clearance between lower foldable strut and rocker arm x_2	$N(u_{x_2}=0.057,\sigma_{x_2}^2=0.010^2)$
Joint clearance between upper link and rocker arm x_3	$N(u_{x_3}=0.039,\sigma_{x_3}^2=0.007^2)$	Joint clearance between main strut and rocker arm x_4	$N(u_{x_4}=0.057,\sigma_{x_4}^2=0.010^2)$
Horizontal assembly deviation of upper foldable strut x_5	$N(u_{x_5}=0,\sigma_{x_5}^2=0.02^2)$	Vertical assembly deviation of upper foldable strut x_6	$N(u_{x_6}=0,\sigma_{x_6}^2=0.1^2)$
Horizontal assembly deviation of main strut x_7	$N(u_{x_7}=0,\sigma_{x_7}^2=0.02^2)$	Vertical assembly deviation of main strut x_8	$N(u_{x_8}=0,\sigma_{x_8}^2=0.1^2)$

According to the reliability design theory [14,20], the kinematic accuracy reliability of the retraction mechanism is expressed as

$$P_r = P(Z>0) = P(\Delta^* - \Delta > 0) \tag{2}$$

It is assumed that the performance function Z obeys the normal distribution [9,26,28,29]. Based on the normal distribution characteristics, Δ^* and Δ also obey the normal distribution. Eq. (2) can be rewritten as

$$P_r = P(\Delta^* - \Delta > 0) = \int_0^{\infty} \frac{1}{\sqrt{2\pi\sigma_Z^2}} exp\left[-\frac{(z-\mu_Z)^2}{2\sigma_Z^2}\right] dz \tag{3}$$

in which,

$$\sigma_Z^2 = \sigma_{\Delta^*}^2 + \sigma_\Delta^2 \text{ and } \mu_Z = \mu_{\Delta^*} - \mu_\Delta \tag{4}$$

Δ is the performance characterization, μ_Δ and σ_Δ^2 are given by the statistical inference method based on the experimental data of the retraction mechanism. However, it should be noted that when dealing with small sample tests, the accuracy and stability of the inference results for μ_Δ and σ_Δ^2 can be challenging to guarantee. This limitation directly affects the stability and reliability of the subsequent reliability calculation results. To overcome this challenge, it is essential to leverage the available prior data effectively to improve the stability of the calculation results. By incorporating prior information, the reliability estimation process can be enhanced, ensuring more dependable and robust results.

3. Kinematic accuracy distribution parameters estimation under small sample

It is difficult to guarantee the accuracy and stability of the inference results of the distribution parameters of performance characterization due to the limited number of retraction tests conducted. To address this issue, the Bayesian method is employed as a reliable approach to fuse prior data and test data. By incorporating prior information into the parameter estimation process, the impact of small sample test conditions on parameter estimation is mitigated, leading to improved stability in the estimation results.

3.1. Bayesian formula

According to the Bayesian formula [6], the parameter estimation expression of the mean μ_Δ and variance σ_Δ^2 of the kinematic accuracy parameter Δ is expressed as

$$\pi(\mu_\Delta, \sigma_\Delta^2|\boldsymbol{T}) \propto p(\boldsymbol{T}|\mu_\Delta, \sigma_\Delta^2)\pi(\mu_\Delta, \sigma_\Delta^2) \tag{5}$$

wherein, $\boldsymbol{T} = [t_1, t_2, \ldots, t_n]$ consists of all test sample values, n denotes the test sample amount, $p(\boldsymbol{T}|\mu_\Delta, \sigma_\Delta^2)$ represents the likelihood function, $\pi(\mu_\Delta, \sigma_\Delta^2)$ represents the prior distribution, and $\pi(\mu_\Delta, \sigma_\Delta^2|\boldsymbol{T})$ represents the posterior distribution.

3.2. Likelihood function

Δ obeys the normal distribution, the likelihood function that combines the test sample information and the overall information can be expressed as

$$p(\boldsymbol{T}|\mu_\Delta, \sigma_\Delta^2) \propto \sigma_\Delta^2\, exp\left(-\alpha\sum_{j=1}^n (t_j-\mu_\Delta)^2\right) =$$

$$\sigma_\Delta^{-n}\exp\{-\alpha[(n-1)s^2 + n(\bar{t}-\mu_\Delta)^2]\} \tag{6}$$

in which,

$$\alpha = \frac{1}{2}\sigma_\Delta^2,\ \ \bar{t} = \frac{1}{n}\sum_{j=1}^n t_j,\ \ s^2 = \frac{1}{n-1}\sum_{j=1}^n (t_j-\bar{t})^2 \tag{7}$$

3.3. Prior distribution

In the case where the test sample obeys the normal distribution with the unknown mean and variance, the joint prior distribution of mean μ_Δ and variance σ_Δ^2 can be assumed to be the normal-inverse gamma distribution [2,3,11], as shown in Eq. (8).

$$\pi(\mu_\Delta,\ \sigma_\Delta^2) = \pi(\mu_\Delta|\sigma_\Delta^2)\pi(\sigma_\Delta^2) = (\sigma_\Delta^2)^{-(\gamma_0+1)} e^{-\left(\frac{\beta_0}{2\sigma_\Delta^2}\right)} \tag{8}$$

in which,

$$\gamma_0 = \frac{(v_0+1)}{2} \text{ and } \beta_0 = v_0{\sigma_0}^2 + k_0(\mu_\Delta - \mu_0)^2 \tag{9}$$

with hyper parameters:

$$\begin{cases} \mu_0 = \overline{\mu_{\Delta p}} \\ k_0 = \dfrac{\overline{\sigma_{\Delta p}^2}}{S_{\mu_{\Delta p}}^2} \\ v_0 = \dfrac{2\left(\overline{\sigma_{\Delta p}^2}\right)^2}{S_{\sigma^2 \Delta p}^2} + 4 \\ {\sigma_0}^2 = \dfrac{v_0 - 2}{v_0}\overline{\sigma_{\Delta p}^2} \end{cases} \tag{10}$$

wherein,

$$\begin{cases} \overline{\mu_{\Delta p}} = \sum_{j=1}^{m} \mu_{\Delta pj} / m \\ S_{\mu_{\Delta p}}^2 = \sum_{j=1}^{m} \left(\mu_{\Delta pj} - \overline{\mu_{\Delta p}}\right)^2 / (m-1) \\ \overline{\sigma_{\Delta p}^2} = \sum_{j=1}^{m} \sigma_{\Delta pj}^2 / m \\ S_{\sigma^2 \Delta p}^2 = \sum_{j=1}^{m} \left(\sigma_{\Delta p}^2 - \overline{\sigma_{\Delta p}^2}\right)^2 / (m-1) \end{cases} \tag{11}$$

Here, $\boldsymbol{M}_{\Delta p} = \left[\mu_{\Delta p1}, \ldots, \mu_{\Delta pm}\right]$ consists of the prior mean sample; $\boldsymbol{\Sigma}_{\Delta p}^2 = \left[\sigma_{\Delta p1}^2, \ldots, \sigma_{\Delta pm}^2\right]$ consists of the prior variance sample; m denotes the prior sample amount.

Typically, hyper parameters can be estimated using historical data and expert knowledge [1,7,24]. In cases where historical data and expert experience are scarce and simulation data is limited, the neural network can be used to expand the simulation data and generate an adequate number of prior samples, thereby obtaining reliable hyper parameters. Section 4 delves into the details of this process.

The joint prior distribution of mean and variance is the normal-inverse gamma distribution, leading to the normal distribution as the prior distribution of μ_Δ conditioned on σ_Δ^2 and the inverse gamma distribution as the prior distribution of σ_Δ^2, as shown in Eq. (12).

$$\begin{cases} \mu_\Delta | \sigma_\Delta^2 \sim N(PN\mu, PN\sigma^2) \\ \sigma_\Delta^2 \sim IGa(PI\alpha, PI\beta) \end{cases} \tag{12}$$

with parameters:

$$\begin{cases} PN\mu = \mu_0, \quad PN\sigma^2 = \dfrac{{\sigma_0}^2}{k_0} \\ PI\alpha = \dfrac{v_0}{2}, \quad PI\beta = \dfrac{v_0 {\sigma_0}^2}{2} \end{cases} \tag{13}$$

To ensure the validity and appropriateness of the prior distribution hypothesis, it is necessary to evaluate the goodness-of-fit of the prior distribution, as detailed in Section 5.

3.4. Posterior distribution

The posterior distribution of mean μ_Δ and variance σ_Δ^2 can be rewritten as

$$\pi(\mu_\Delta, \sigma_\Delta^2 | \boldsymbol{T}) = (\sigma_\Delta^2)^{-(\gamma_n + 1)} e^{-(\beta_n / 2\sigma_\Delta^2)} \tag{14}$$

in which,

$$\gamma_n = (v_n + 1)/2 \text{ and } \beta_n = v_n {\sigma_n}^2 + k_n(\mu_\Delta - \mu_n)^2 \tag{15}$$

with posterior distribution parameters:

$$\begin{cases} \mu_n = \dfrac{k_0}{k_0 + n}\mu_0 + \dfrac{n}{k_0 + n}\bar{t} \\ k_n = k_0 + n \\ v_n = v_0 + n \\ v_n {\sigma_n}^2 = v_0 \sigma_0^2 + (n-1)s^2 + \dfrac{k_0 n}{k_0 + n}(\mu_0 - \bar{t})^2 \end{cases} \tag{16}$$

3.5. Point estimation based on posterior distribution

The maximum likelihood estimation method is employed to estimate the posterior distribution integrating overall information, sample information, and prior information, as shown in Eq. (17).

$$\begin{cases} \dfrac{\partial \pi(\mu_\Delta, \sigma_\Delta^2 | \mathrm{T})}{\partial \mu_\Delta} = 0 \\ \dfrac{\partial \pi(\mu_\Delta, \sigma_\Delta^2 | \mathrm{T})}{\partial \sigma_\Delta^2} = 0 \end{cases} \tag{17}$$

The point estimate values for the kinematic accuracy distribution parameters $\hat{\mu}_\Delta$ and $\hat{\sigma}_\Delta^2$ are finally derived as

$$\begin{cases} \hat{\mu}_\Delta = \mu_n \\ \hat{\sigma}_\Delta^2 = \dfrac{v_n {\sigma_n}^2}{v_n + 3} \end{cases} \tag{18}$$

By substituting $\hat{\mu}_\Delta$ and $\hat{\sigma}_\Delta^2$ into Eq. (3), the kinematic accuracy reliability of the retraction mechanism is obtained.

4. Kinematic accuracy reliability estimation process fusing prior and test samples

The kinematic accuracy reliability estimation process by integrating prior information and test information is depicted in Fig. 8. The following parts provide a detailed overview of the research methodology.

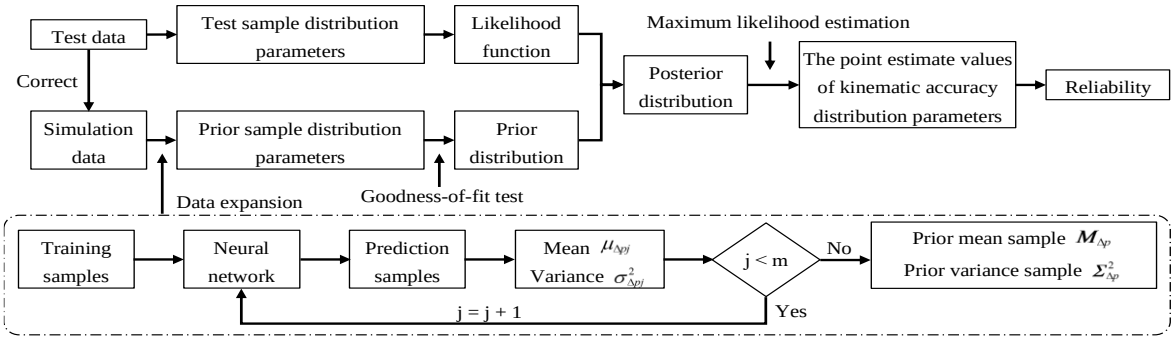

Fig. 8. Reliability estimation flow chart under small sample.

4.1. Hyper parameter determination method based on neural network

Expert experience, historical data, and similar product data are commonly used to estimate hyper parameters. However, when these approaches are not feasible due to data scarcity, the data expansion capability of the neural network [8,19] can be leveraged as a complementary solution. In this research, the simulation data is used as the training sample for the BP neural network. The trained neural network is then utilized to generate prediction samples, which are used to generate prior mean and prior variance samples. These samples facilitate the estimation of hyper parameters, thereby overcoming the limitations imposed by insufficient prior information.

The process of expanding prior samples and determining hyper parameters involves several steps.

1) Random sample m_0 sets of test points that conform to the distribution characteristics of the random variables and invoke the mechanism dynamic simulation model to perform batch simulations, resulting in corresponding response data for each set, which constitute the initial prior samples $\boldsymbol{T}^0 = [t_1^0, t_2^0, \ldots, t_{m_0}^0]$.
2) Design and train the BP neural network using the m_0 sets of simulated data points and corresponding response results, as illustrated in Fig. 9. To ensure model fitting accuracy and prevent overfitting, various parameters such as activation functions, training algorithms, the number of hidden layers, the number of neurons in each hidden layer, the number of epochs, dataset proportions, learning rates, training objectives, and momentum factors can be adjusted to achieve an optimal neural network. The Mean Square Error (MSE) serves as the evaluation metric for neural network training effectiveness [5]. When MSE $\leq 1\times10^{-6}$, the neural network is considered a high-precision surrogate model suitable for subsequent calculations of mechanism kinematic accuracy reliability.

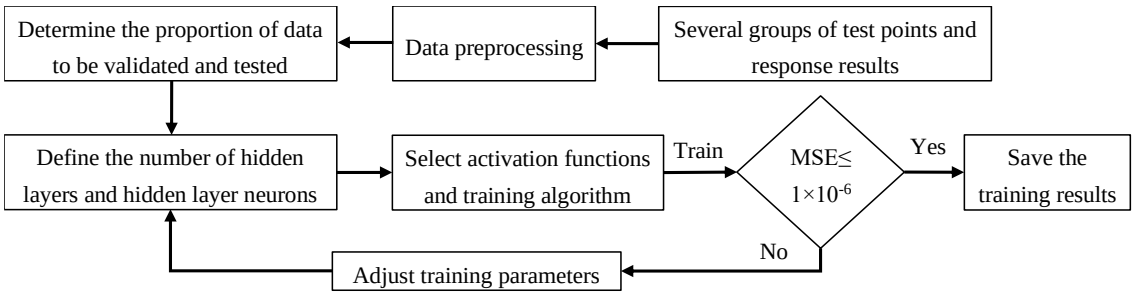

Fig. 9. Neural network training flow chart.

3) Generate m_s sets of prediction test points based on the distribution information of random variables, input them into the neural network, and obtain m_s sets of corresponding response results, i.e., prediction samples $\boldsymbol{T}^s = [t_1^s, t_2^s, \ldots, t_{m_s}^s]$.
4) Calculate the mean $\mu_{\Delta pj}$ and variance $\sigma_{\Delta pj}^2$ of the prediction samples $\boldsymbol{T}^s$.
5) Repeat steps 3) - 4) m times. The prior mean samples $\boldsymbol{M}_{\Delta p}$ consist of m sets of means derived from the prediction samples, while the prior variance samples $\boldsymbol{\Sigma}_{\Delta p}^2$ consist of m sets of variances obtained from the prediction samples. The expansion of the prior sample data is now finalized.
6) Solve the hyper parameter values based on the sample $\boldsymbol{M}_{\Delta p}$ and $\boldsymbol{\Sigma}_{\Delta p}^2$, determine the prior normal distribution parameter values and the prior inverse gamma parameter values, and then complete the hyper parameter estimation.
7) Verify the rationality of the prior distribution hypothesis using the K-S goodness of fit test method.

4.2. Kinematic accuracy reliability estimation process

Based on the results of hyper parameter estimation, the determination process of the kinematic accuracy reliability estimation is as follows:

1) Calculate the test statistic values $\bar{t}$ and s^2 based on the small sample test data $\boldsymbol{T}$.
2) Substitute the hyper parameter values containing prior information and the test statistic values containing test information into Eq. (16), and obtain the posterior distribution parameters μ_n, k_n, v_n, and ${\sigma_n}^2$.
3) Substitute μ_n, k_n, v_n, and ${\sigma_n}^2$ into Eq. (18), and obtain

the point estimate values for kinematic accuracy distribution parameters $\hat{\mu}_{\Delta}$ and $\hat{\sigma}_{\Delta}^2$.

4) Substitute $\hat{\mu}_{\Delta}$ and $\hat{\sigma}_{\Delta}^2$ into Eq. (3) to derive the kinematic accuracy reliability of the retraction mechanism.

5. Kinematic accuracy reliability estimation of retraction mechanism

The proposed method is verified for its feasibility and effectiveness by applying it to estimate the kinematic accuracy reliability of a new type of complex rotatable tire landing gear retraction mechanism. Through the utilization of prediction samples generated by the trained neural network and the Bayesian method, the challenges of difficult hyper parameter estimation and low stability in the estimation results of kinematic accuracy reliability, caused by factors such as limited field test data and insufficient prior information, are successfully addressed.

5.1. Kinematic accuracy reliability estimation of retraction mechanism

The parameters required for reliability evaluation of the retraction mechanism are presented in Table 2. To gather the necessary data for the analysis, both real and simulation tests of the retraction mechanism have been conducted. The test sample data are provided in Table 3, and the simulation data used to train the neural network are shown in Table 4.

Table 2. Reliability evaluation parameters of retraction mechanism.

$n = 10$	$m_0 = 500$
$m_s = 80$	$m = 3000$
$\Delta^* \sim N(0.2, 0.02^2)$	/

Table 3. Test sample data $\boldsymbol{T}$.

Serial number	$\boldsymbol{T}$/(°)	Serial number	$\boldsymbol{T}$/(°)
1	0.048	6	0.062
2	0.023	7	0.009
3	0.042	8	0.032
4	0.026	9	0.002
5	0.032	10	0.070

Table 4. Simulation data $\boldsymbol{T}^0$.

Serial number	$\boldsymbol{T}^0$/(°)	Serial number	$\boldsymbol{T}^0$/(°)
1	0.043	251	0.085
…		…	
250	0.063	m_0	0.071

(1) Train the neural network

After generating 500 test points based on the distribution information in Table 1, the simulation model is invoked to perform batch simulations, resulting in corresponding rotation angle errors as shown in Table 4. Using structural clearances and assembly deviations as inputs and rotation angle errors as responses, a BP neural network with one hidden layer is created. To ensure model fitting accuracy, the Levenberg-Marquardt training algorithm is employed, and the number of neurons in the hidden layer is set to 10. The activation function for the hidden layer is the hyperbolic tangent sigmoid function, while the output layer employs a linear function. To avoid overfitting, the training data input into the network is divided into three groups, with 70% for the training sample set and 15% each for the validation and test sample sets. The regression performance of the neural network and the error histogram are illustrated in Fig. 10 and Fig. 11.

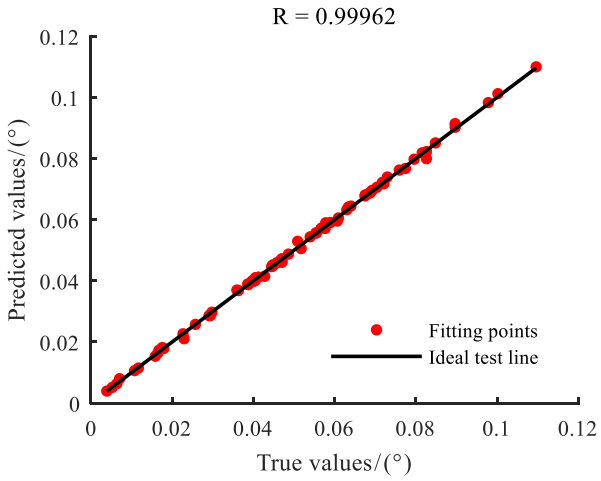

Fig. 10. Comparison of true and predicted values.

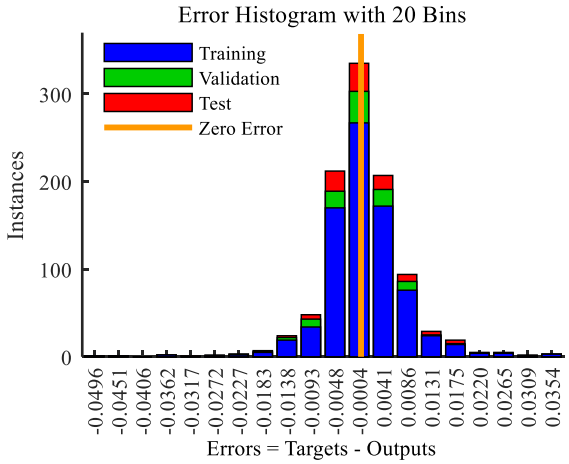

Fig. 11. Error histogram.

The model's regression coefficient is 0.99962, and the mean square error is 5.579×10^{-7}, which falls below the threshold 1×10^{-6}. The majority of errors fall within the range of -0.009 to 0.008, with a maximum error range between -0.050 and 0.035.

This model accurately reflects the landing gear retraction mechanism's kinematic accuracy variations with changes in structural clearances and assembly deviations, thus indicating the successful completion of neural network training.

(2) Generate prior sample data

Using the random distribution information in Table 1, m_s groups of test points are generated and subsequently input into the neural network to generate a corresponding set of prediction samples. The mean $\mu_{\Delta pj}$ and variance $\sigma^2_{\Delta pj}$ are then calculated based on these prediction samples. This process is repeated m times to generate the prior mean samples $\boldsymbol{M}_{\Delta p}$ and prior variance samples $\boldsymbol{\Sigma}^2_{\Delta p}$, as presented in Table 5.

Table 5. Prior sample data.

Serial number	Prior sample type	Prior sample values
1	$\mu_{\Delta p1}$	0.036
	$\sigma^2_{\Delta p1}$	3.691×10^{-4}
2	$\mu_{\Delta p2}$	0.034
	$\sigma^2_{\Delta p2}$	4.861×10^{-4}
…	…	…
m	$\mu_{\Delta pm}$	0.038
	$\sigma^2_{\Delta pm}$	3.329×10^{-4}

Based on the data in Table 5, the frequency distribution histograms of the prior samples are depicted in Fig. 12. It can be seen that the frequency distribution of prior mean samples exhibits characteristics similar to the normal distribution, while the frequency distribution of prior variance samples demonstrates characteristics akin to the inverse gamma distribution. This qualitative assessment supports the reasonableness of the prior distribution hypothesis.

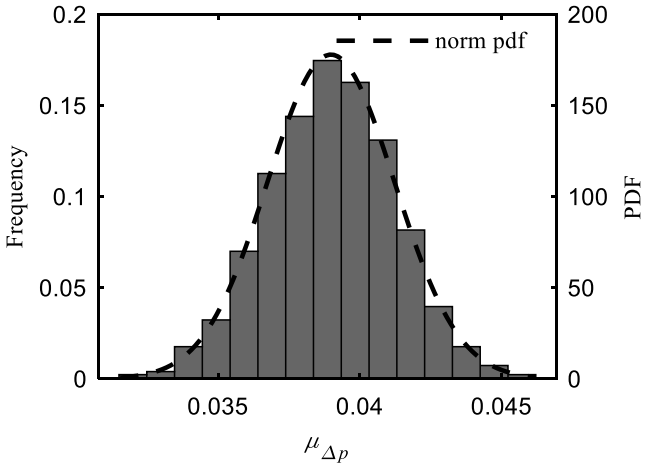

(a) Frequency distribution histogram of mean

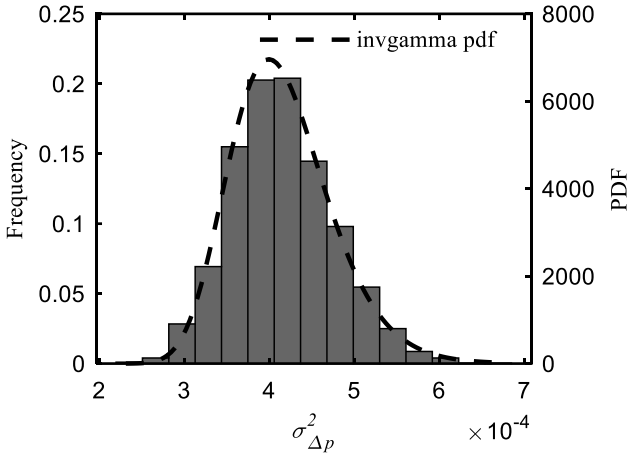

(b) Frequency distribution histogram of variance

Fig. 12. Frequency distribution histograms of prior samples.

(3) Estimate hyper parameters

The prior sample data in Table 5 are used to calculate the estimate values of the hyper parameters, as indicated in Table 6, by substituting into Eq. (10). In order to assess the goodness-of-fit of the prior distribution hypothesis, a K-S (Kolmogorov-Smirnov) goodness-of-fit test is conducted, and the results are displayed in Table 7.

Table 6. The hyper parameters of the prior distribution.

μ_0	0.039
k_0	82.775
v_0	99.606
σ_0^2	4.078×10^{-4}

Table 7. The goodness of fit test of the prior distribution.

Distribution	P-value	Test statistic	Significance level	Critical value
$N(PN\mu, PN\sigma^2)$	0.662	0.013	5%	0.025
$IGa(PI\alpha, PI\beta)$	0.157	0.021	5%	0.025

The P-values associated with the prior normal distribution and prior inverse gamma distribution are observed to exceed the significance level, and the corresponding test statistics are found to be smaller than the critical value. These results indicate that there is sufficient evidence to accept the hypothesis that the assumed distributions accurately represent the underlying parameters. By conducting a quantitative analysis, the rationality of the prior distribution hypothesis is further confirmed.

The test sample data in Table 3 and the hyper parameters in Table 6 are brought into Eq. (16) to obtain the hyper parameters of the posterior distribution, as shown in Table 8. Substituting the hyper parameters in Table 8 into Eq. (18), the point estimate

values for the kinematic accuracy distribution parameters are obtained. $\hat{\mu}_{\Delta} = 0.0385$, $\hat{\sigma}_{\Delta}^2 = 3.989 \times 10^{-4}$.

Table 8. The hyper parameters of the posterior distribution.

μ_n	0.0385
k_n	92.775
v_n	109.606
σ_n^2	4.098×10^{-4}

As depicted in Fig. 13 and Fig. 14, visual representations of the prior and posterior distributions, as well as the maximum posterior estimation for the mean μ_{Δ} and variance σ_{Δ}^2, are presented.

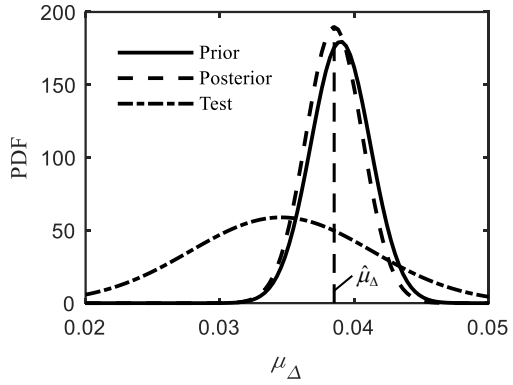

Fig. 13. A schematic diagram of the prior distribution, posterior distribution, and maximum posterior estimation of mean.

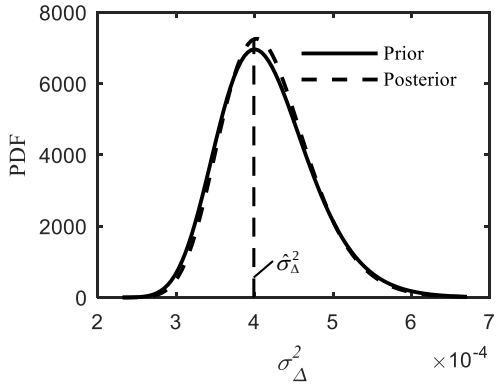

Fig. 14. A schematic diagram of the prior distribution, posterior distribution, and maximum posterior estimation of variance.

It is evident that the incorporation of prior information has led to a discernible increment in the mean of kinematic accuracy mean, accompanied by a reduction in the standard deviation. However, the distribution pattern of kinematic accuracy variance exhibits relatively minor changes. These observations collectively underscore the influence and effectiveness of prior information on the estimation of kinematic accuracy parameters.

(4) Kinematic reliability estimation of retraction mechanism

The kinematic accuracy point estimate values $\hat{\mu}_{\Delta}$ and $\hat{\sigma}_{\Delta}^2$ are brought into Eq. (3), in which $\mu_Z = 0.1615$, $\sigma_Z^2 = 7.989 \times 10^{-4}$. The resulting reliability of the kinematic accuracy of the retraction mechanism is determined to be 99.9999994%.

5.2. Stationarity test

(1) Stationarity test of prior sample values

To assess the stability and accuracy of the generated prior samples and ensure the reliability of subsequent calculations, a quantitative analysis is conducted. The curves of the prior mean $\mu_{\Delta pj}$ and prior variance $\sigma_{\Delta pj}^2$ with the amount of prediction data are shown in Fig. 15.

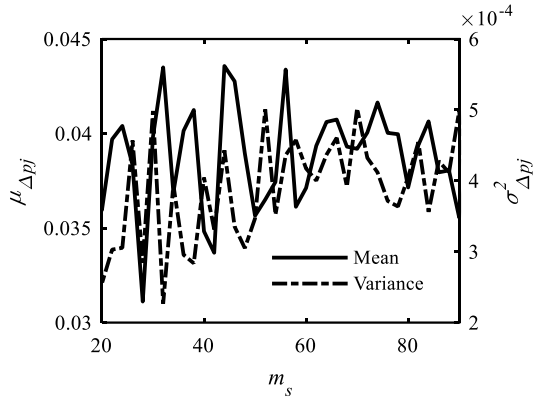

Fig. 15. Curve of prior sample values changing with the prediction data amount.

It can be seen that the fluctuation amplitudes of $\mu_{\Delta pj}$ and $\sigma_{\Delta pj}^2$ gradually decrease as m_s increases. When $m_s = [60,90]$, the fluctuation amplitudes of $\mu_{\Delta pj}$ and $\sigma_{\Delta pj}^2$ become stable. The curves of the standard deviation $SD\mu_{\Delta pj}$ of the prior mean sample and the standard deviation $SD\sigma_{\Delta pj}^2$ of the prior variance sample with the amount of prediction data are shown in Fig. 16.

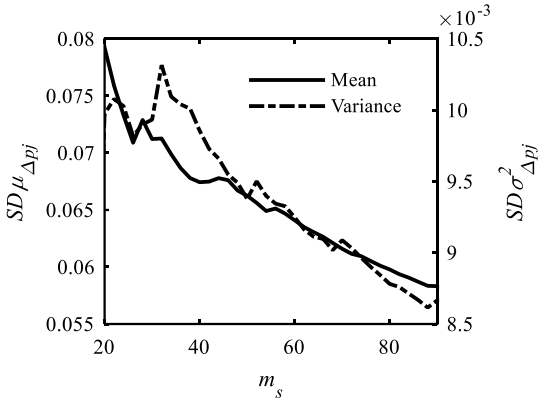

Fig. 16. Stationarity analysis of prior sample values.

When $m_s \geq 40$, it can be seen that $SD\mu_{\Delta pj}$ and $SD\sigma_{\Delta pj}^2$ exhibit a steady decrease as m_s increases. When $m_s = 80$,

$SD\mu_{\Delta pj} = 5.978 \times 10^{-2}$, $SD\sigma^2_{\Delta pj} = 8.781 \times 10^{-3}$, satisfying the requirements.

Therefore, with the aim of maintaining stable calculation results while enhancing computational efficiency, m_s is set to 80.

(2) Stationarity analysis of prior distribution parameters

To assess the stationarity of the prior distribution parameters, a quantitative analysis is conducted using the example of the prior inverse gamma distribution parameters. The curves depicting the shape parameter $PI\alpha$ and scale parameter $PI\beta$ of the prior inverse gamma distribution with the prior sample amount are shown in Fig. 17.

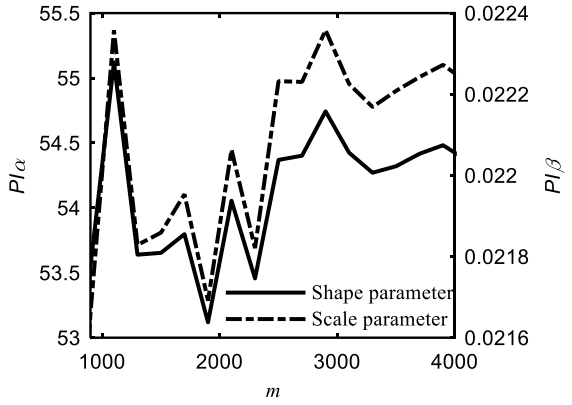

Fig. 17. Curve of prior distribution parameters changing with the prior sample amount.

It can be seen that the fluctuation amplitudes of $PI\alpha$ and $PI\beta$ decrease gradually as m increases. When $m =$ [2500,5000], the curves exhibit stability. The variation curves of the standard deviation of the shape parameter $SDPI\alpha$ and the standard deviation of the scale parameter $SDPI\beta$ with the prior sample amount m are shown in Fig. 18.

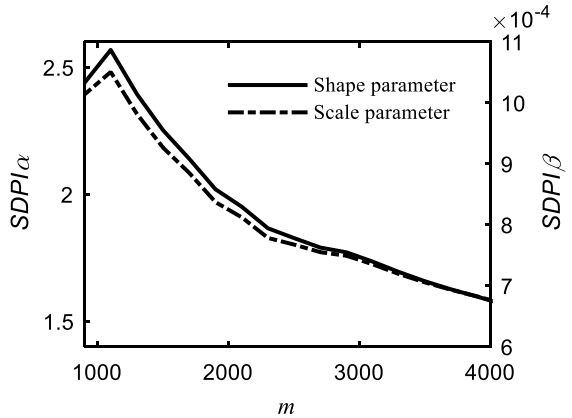

Fig. 18. Stationarity analysis of prior distribution parameters.

When $m \geq 1100$, both $SDPI\alpha$ and $SDPI\beta$ show a steady decrease as m increases. When $m = 3000$, $SDPI\alpha = 1.771$, $SDPI\beta = 7.49 \times 10^{-4}$, which can satisfy the use requirement.

As a result, m is set to 3000 in order to increase computation efficiency under the presumption of maintaining the stability of the calculation results.

(3) Stationarity analysis of kinematic accuracy distribution parameters

The estimate values of the kinematic accuracy distribution parameters and the variation in these parameters with changes in the number of test samples and prior samples are illustrated in Fig. 19 and Fig. 20. When the number of prior samples falls within the range of [2500, 4000], the estimation results for the kinematic accuracy distribution parameters exhibit minimal fluctuations.

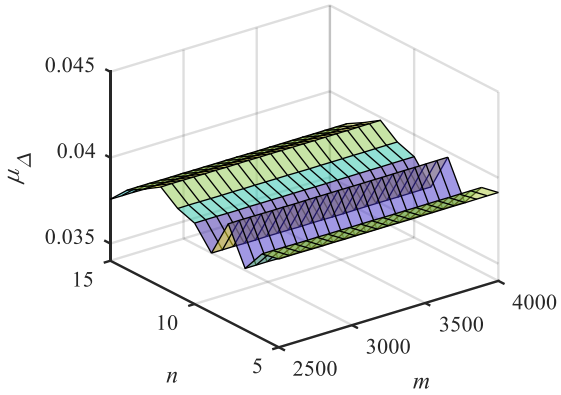

Fig. 19. Three-dimensional graph of mean estimation results.

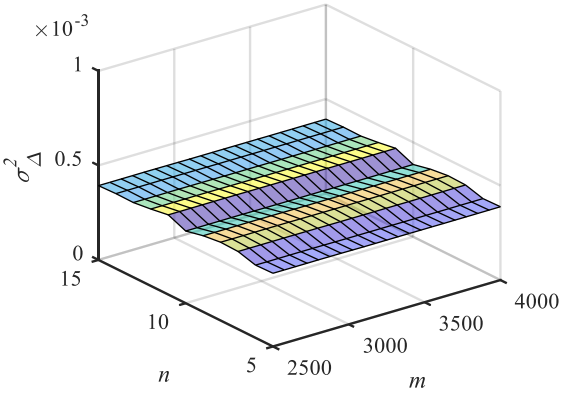

Fig. 20. Three-dimensional graph of variance estimation results.

In order to assess the effectiveness of the proposed method, a comparison is made with the classical interval estimation method [23] using a confidence coefficient of 0.95. The analysis focuses on the variation trends of the kinematic accuracy distribution parameters, μ_Δ and σ^2_Δ, of the retraction mechanism. The test sample amount is varied within the range of [5, 15]. The calculation results are presented in Fig. 21 and Fig. 22.

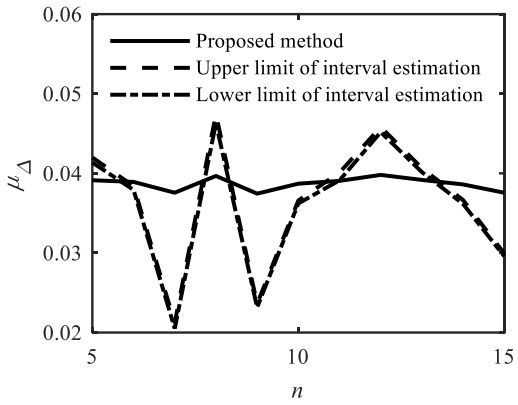

Fig. 21. Curve of mean estimation results with the change in test sample amount.

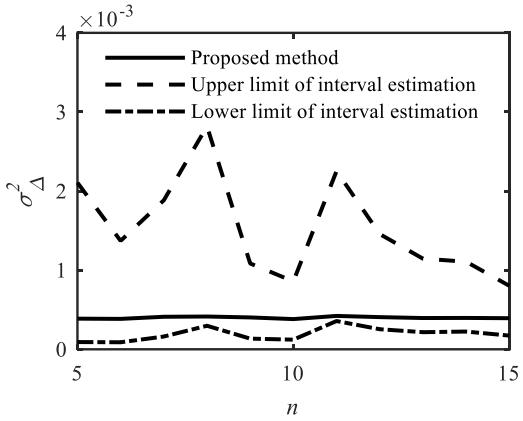

Fig. 22. Curve of variance estimation results with the change in test sample amount.

As presented in Table 9, the fluctuation amplitudes of the kinematic accuracy distribution parameters are shown. It is evident that the fluctuation amplitude obtained through our proposed methodology is less than 10% of that acquired using the classical interval estimation method.

Table 9. The fluctuation amplitudes of the estimation results.

Estimation results	μ_Δ	σ_Δ^2	p_f
Proposed method	0.0024	4.015×10^{-5}	5.900×10^{-9}
Upper limit of interval estimation	0.0262	0.002	0.0034
Lower limit of interval estimation	0.0258	2.684×10^{-4}	3.804×10^{-9}

The proposed method is significantly better than the classical interval estimation method in the stability of the estimation results of μ_Δ and σ_Δ^2 by fusing prior samples. The robustness of the proposed method under the condition of small sample is proved. Furthermore, the amplitude variation of the estimation results obtained with the proposed method falls within the range of the amplitude variation observed in the interval estimation results, thereby attesting to the accuracy of the proposed method under the condition of small sample.

In addition, the mean estimation results of the kinematic accuracy parameter calculated by the proposed method fall within the upper range of the mean estimation interval derived from the classical interval estimation method relying solely on the test data. Similarly, the variance estimation results fall within the lower range of the variance estimation interval. These findings suggest that the proposed method possesses a corrective effect on the estimation results of distribution parameters under small-sample test conditions.

As illustrated in Fig. 23, the failure probabilities derived from this method fall within the range obtained through classical interval estimation, exhibiting minimal fluctuation.

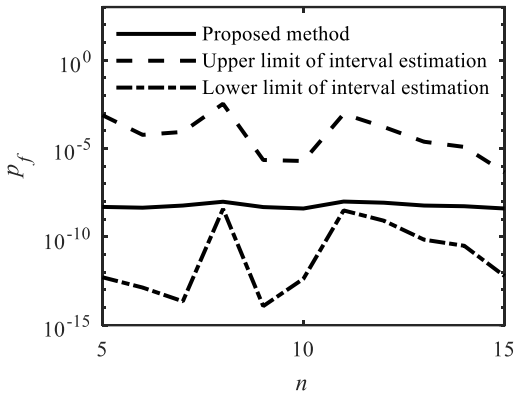

Fig. 23. Curve of failure probability with the change in test sample amount.

It is evident that, due to the propagation of errors in the calculation process, the fluctuations in the results yielded by interval estimation become less tenable. This underscores the stability of the reliability analysis results obtained through this method, particularly under small sample conditions.

5.3. Influences of uncertainty factors on kinematic accuracy reliability

The joint clearances and assembly deviations undoubtedly have an impact on the kinematic accuracy of the retraction mechanism during its operational lifespan. In order to improve the kinematic accuracy reliability of the retraction mechanism, the influence analysis of the uncertainty factors of the retraction mechanism is carried out. The relationship between the distribution parameters of random variables and reliability is depicted in Fig. 24 and Fig. 25.

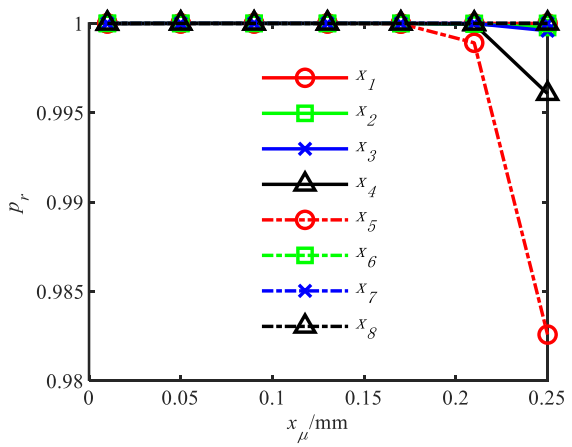

Fig. 24. The relationship diagram between the mean value of random variables and reliability.

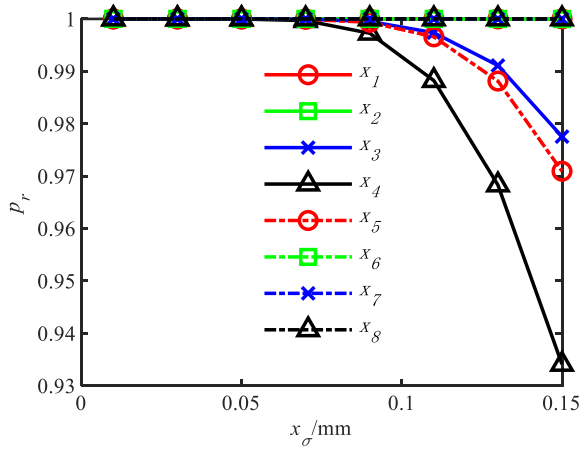

Fig. 25. The relationship diagram between the standard deviation of random variables and reliability.

It is evident that the joint clearance between the rocker arm and the upper link x_3, the joint clearance between the rocker arm and the main strut x_4, and the horizontal installation deviation of the upper foldable strut x_5 are the primary factors influencing the kinematic accuracy reliability of the retraction mechanism. Reducing the mean value of x_5 and x_4 can effectively improve the kinematic accuracy reliability of the retraction mechanism. Hence, during the design phase, it is crucial to ensure that x_5 is controlled within the range of 0 ~ 0.15 mm and x_4 is limited to the range of 0 ~ 0.02 mm. Additionally, during the subsequent maintenance process, it is recommended to prioritize inspections and evaluations of the variations in x_3, x_4, and x_5 to monitor and address any potential deviations from the desired values. By addressing these key factors, the overall kinematic accuracy reliability of the retraction mechanism can be improved and maintained at an optimal level.

5.4. Limitations of kinematic accuracy reliability estimation method

(1) Accuracy of simulation and neural network models

The approach heavily relies on prior data. If the simulation model cannot accurately represent the real system, or if the neural network model fails to capture the system's highly nonlinear behavior adequately, it can result in inaccurate prior samples. Consequently, this can lead to compromised reliability estimation results.

(2) Prior distribution hypothesis for performance characteristics

The Bayesian method assumes that the prior distribution accurately reflects prior knowledge. If the prior distribution lacks a clear specification or if the prior samples obtained through the neural network cannot qualitatively and quantitatively validate the rationality of the prior distribution hypothesis, it may introduce bias into the reliability estimation results.

This methodology is particularly suitable for static reliability analysis of mechanisms under small-sample test conditions during the development of new products. Moreover, in the operational phase of the mechanism, this approach can be employed to assess reliability by means of detecting joint clearances and assembly deviations, thereby offering valuable insights to maintenance engineers. However, it requires further refinement and adaptation for time-dependent reliability analysis, especially for systems with complex nonlinear behaviors, during the operational phase. Further improvements are necessary to extend its applicability to complex, nonlinear, and time-dependent systems.

6. Conclusion

(1) The key innovations of this research lie in the integration of the data expansion capability of the neural network with the robust statistical foundation of the Bayesian method. This distinctive integration empowers the generation of an extensive array of prior samples characterized by their precision and stability, as assured through rigorous stationarity analyses. This approach effectively mitigates the challenges associated with acquiring sufficient prior information, such as expert experience and historical data, which are often elusive, particularly in the context of novel product development.

(2) In this study, a kinematic accuracy reliability estimation method based on the Bayesian method is proposed to analyze the kinematic accuracy reliability of the retraction mechanism. Through the analysis, it is observed that the joint clearance between the rocker arm and the upper link, the joint clearance between the rocker arm and the main strut, and the horizontal assembly deviation of the upper foldable strut significantly influence the kinematic reliability of the retraction mechanism. These findings highlight the critical factors that should be carefully controlled and monitored in order to enhance the overall kinematic accuracy reliability of the retraction mechanism.

(3) The proposed parameter estimation method, which incorporates prior information, demonstrates its ability to improve the estimation results compared to the classical interval estimation method under the condition of small sample. Furthermore, the stability of the estimation results obtained through the proposed method is significantly superior to that of the classical interval estimation method. These findings highlight the effectiveness of incorporating prior information in improving estimation accuracy and stability under small sample conditions, offering valuable insights for reliable parameter estimation in various fields of research and application.

(4) The proposed method presents a valuable approach for estimating the kinematic accuracy reliability of similar products in situations where there is a scarcity of test samples and limited availability of expert experience and historical data. Future research endeavors will extend to explore and validate the applicability of this method in analyzing the static reliability and time-dependent reliability of other performance characteristics in mechanisms. This will facilitate more precise and reliable performance reliability estimation for similar products under conditions of constrained data resources.

Acknowledgments

This study was supported by the National Natural Science Foundation of China (52172368, 52275114, 52302453), the Natural Science Foundation of Jiangsu Province (BK20220135), the Research Fund of State Key Laboratory of Mechanics and Control of Mechanical Structures (Nanjing University of Aeronautics and Astronautics) (Grant No. MCMS-I-0221Y02)).

References

1. Belinda P, Stanley L, Ian J M et al. Robust Hyperparameter Estimation Protects against Hypervariable Genes and Improves Power to Detect Differential Expression. The Annals of Applied Statistics 2016; 10(2):946-963, https://doi.org/10.1214/16-AOAS920.
2. Cai M, van Buuren S, Vink G. Joint Distribution Properties of Fully Conditional Specification under the Normal Linear Model with Normal Inverse-Gamma Priors. Scientific Reports 2023; 13(1):644, https://doi.org/10.1038/s41598-023-27786-y.
3. Chan J C C. Asymmetric Conjugate Priors for Large Bayesian Vars. Quantitative Economics 2022; 13(3):1145-1169, https://doi.org/https://doi.org/10.3982/QE1381.
4. Currey N S. Aircraft Landing Gear Design: Principles and Practices. 1988. https://doi.org/10.2514/4.861468.
5. Deng J, Gu D, Li X et al. Structural Reliability Analysis for Implicit Performance Functions Using Artificial Neural Network. Structural Safety 2005; 27(1):25-48, https://doi.org/10.1016/j.strusafe.2004.03.004.
6. Devore J L. Probability and Statistics for Engineering and the Sciences. Calgary, Cengage Learning: 2007: 72-74.
7. Dunlop M M, Helin T, Stuart A M. Hyperparameter Estimation in Bayesian Map Estimation: Parameterizations and Consistency. The SMAI journal of computational mathematics 2020; 6:69-100, https://doi.org/10.5802/smai-jcm.62.
8. Farrell M, Recanatesi S, Moore T et al. Gradient-Based Learning Drives Robust Representations in Recurrent Neural Networks by Balancing Compression and Expansion. Nature Machine Intelligence 2022; 4(6):564-573, https://doi.org/10.1038/s42256-022-00498-0.
9. Feliu-Talegon D, Feliu-Batlle V. A Fractional-Order Controller for Single-Link Flexible Robots Robust to Sensor Disturbances. IFAC-PapersOnLine 2017; 50(1):6043-6048, https://doi.org/10.1016/j.ifacol.2017.08.1450.
10. Gao J, An Z, Liu B. A New Method for Obtaining P-S-N Curves under the Condition of Small Sample. Proceedings of the Institution of Mechanical Engineers, Part O: Journal of Risk and Reliability 2017; 231(2):130-137, https://doi.org/10.1177/1748006X16686896.
11. Hamada M S, Wilson A G, Reese C S et al. Bayesian Reliability. Berlin, Springer: 2008: 47-48. https://doi.org/10.1007/978-0-387-77950-8.

12. Hongzhou L, Lixia S. Reliability Parameter Interval Estimation of Nc Machine Tools Considering Working Conditions. Mathematical Problems in Engineering 2017; 2017:1-7, https://doi.org/10.1155/2017/4037903.
13. Hu H H, Wang P, Zhou H Y. Sequential Reliability Analysis for the Adjusting Mechanism of Tail Nozzle Considering Wear Degradation. Machines 2022; 10(8), https://doi.org/10.3390/machines10080613.
14. Jardine A K, Tsang A H. Maintenance, Replacement, and Reliability: Theory and Applications. CRC Press: 2021. https://doi.org/10.1201/9780429021565.
15. Ke Z, Zhou W. Parameter Estimation Model of Small Test Samples Based on Grey Bootstrap Method and Unascertained Rational Number. Binggong Xuebao/Acta Armamentarii 2019; 40(4):874-879, https://doi.org/10.3969/j.issn.1000-1093.2019.04.023.
16. Li H Y, Xie L Y, Liu J et al. Reliability Evaluation of Bearings in Theintelligent Robot for Changing the Hobwithout Failure Data. Journal of Mechanical Engineering 2019; 55(2):186-194, https://doi.org/10.3901/jme.2019.02.186.
17. Li X Y, Chen W B, Kang R. Performance Margin-Based Reliability Analysis for Aircraft Lock Mechanism Considering Multi-Source Uncertainties and Wear. Reliability Engineering & System Safety 2021; 205:107234, https://doi.org/10.1016/j.ress.2020.107234.
18. Liu J, Ren Y. A General Transfer Framework Based on Industrial Process Fault Diagnosis under Small Samples. IEEE Transactions on Industrial Informatics 2021; 17(9):6073-6083, https://doi.org/10.1109/TII.2020.3036159.
19. Medjber A, Guessoum A, Belmili H et al. New Neural Network and Fuzzy Logic Controllers to Monitor Maximum Power for Wind Energy Conversion System. Energy 2016; 106:137-146, https://doi.org/10.1016/j.energy.2016.03.026.
20. Melchers R E, Beck A T. Structural Reliability Analysis and Prediction. John Wiley & Sons: 2018. https://doi.org/10.1002/9781119266105
21. Peng C, Cai Y, Liu G et al. Developing a Reliability Model of Cnc System under Limited Sample Data Based on Multisource Information Fusion. Mathematical Problems in Engineering 2020; 2020:1-10, https://doi.org/10.1155/2020/3645858.
22. Qiu W, Tang Q, Teng Z et al. Failure Rate Prediction of Electrical Meters Based on Weighted Hierarchical Bayesian. Measurement 2019; 142:21-29, https://doi.org/10.1016/j.measurement.2019.04.062.
23. Stepień B. A Comparison of Classical and Bayesian Interval Estimation for Long-Term Indicators of Road Traffic Noise. Acta Acustica united with Acustica 2018; 104(6):1118-1129, https://doi.org/10.3813/AAA.919276.
24. van de Schoot R, Depaoli S, King R et al. Bayesian Statistics and Modelling. Nature Reviews Methods Primers 2021; 1(1), https://doi.org/10.1038/s43586-020-00001-2.
25. Wang R, Chen H, Dong Y et al. Reliability Analysis and Optimization of Dynamics of Metamorphic Mechanisms with Multiple Failure Modes. Applied Mathematical Modelling 2023; 117:431-450, https://doi.org/10.1016/j.apm.2022.12.023.
26. Wang X, Geng X, Wang L et al. Motion Error Based Robust Topology Optimization for Compliant Mechanisms under Material Dispersion and Uncertain Forces. Structural and Multidisciplinary Optimization 2018; 57(6):2161-2175, https://doi.org/10.1007/s00158-017-1847-5.
27. Yin Y, Nie H, Ni H J et al. Reliability Analysis of Landing Gear Retraction System Influenced by Multifactors. Journal of Aircraft 2016; 53(3):713-724, https://doi.org/10.2514/1.C033333.
28. Zhan Z H, Zhang X M, Zhang H D et al. Unified Motion Reliability Analysis and Comparison Study of Planar Parallel Manipulators with Interval Joint Clearance Variables. Mechanism and Machine Theory 2019; 138:58-75, https://doi.org/10.1016/j.mechmachtheory.2019.03.041.
29. Zhang J, Xiao M, Gao L. A New Method for Reliability Analysis of Structures with Mixed Random and Convex Variables. Applied Mathematical Modelling 2019; 70:206-220, https://doi.org/10.1016/j.apm.2019.01.025.
30. Zhao Q, Jia X, Cheng Z et al. Bayesian Estimation of Residual Life for Weibull-Distributed Components of on-Orbit Satellites Based on Multi-Source Information Fusion. Applied Sciences 2019; 9(15), https://doi.org/10.3390/app9153017.